We thank the reviewer for acknowledging the improvements made in our revised manuscript. We appreciate the constructive feedback and have further clarified and emphasized the key points as suggested. The following table provides a point-by-point response to each comment, outlining the corresponding changes and improvements made in the manuscript.

## Comment

Morphological confirmation. It would be helpful to specify on which day of the experiment these samples were collected for imaging. SEM imaging for each collection day could also be helpful if no other supporting analysis is available.

Regarding the relationship between turbidity and coccoliths, the main point is that there is no direct evidence confirming the presence of coccoliths. I'm uncertain how the data for Fig. 5c were obtained; if the authors explain they used a > 10 μm filtration in flow cytometry, the size classes shown (3-4 and 5-10  $\mu$ m) are smaller than that. Could you clarify this discrepancy? Additionally, unless there is direct proof that these are indeed coccoliths in the 3-4 μm size fraction, they should refrain from concluding that they

## Response

We agree that continuous SEM sampling would have been beneficial for tracking morphological changes throughout the experiment. However, the samples for SEM imaging were taken on the day before the end of the experiment (15 June 2023). Initially, SEM imaging was not part of the experimental plan, as it was expected that larger phytoplankton would dominate the bloom. Thus, these samples were taken as an additional measurement of opportunity rather than as part of a pre-defined sampling schedule.

We have clarified this point and revised the respective Methods (Lines 262–264) and Results (Lines 463–475) sections in the manuscript for clarity.

Direct evidence for the presence of coccoliths is provided by the SEM images shown in the supplement (Figure S6, panel c). The high density of coccoliths visible in this image indicates their abundance in the water column, at least toward the end of the experiment when this sample was taken. This observation, in turn, supports the presence of *Emiliania huxleyi* as the producer of these coccoliths.

Regarding the data from which we got information about the bloom composition, there appears to have been a misunderstanding, which we now clarify. We used several complementary instruments and methods:

 A FlowCam (not a flow cytometer), providing images of the individual particles; are coccoliths (also in the caption of Fig. 5). I agree that this is closely related to the presence of coccoliths, as indicated in the literature, but the fact that you cannot observe them in flow cytometry while still obtaining this data is perplexing. For example, other factors that cause turbidity could be the biofilm of bloom-related microorganisms or other flocs obtained from the oxidation of an organic-rich environment.

- 2. A LISST200X, deriving particle-size distributions from forward light scattering; and
- 3. HPLC-derived quantifying marker pigments concentrations.

From FlowCam imaging, we obtained direct evidence for the presence of certain phytoplankton taxa. We identified the diatom *Cylindrotheca closterium* as one of the two dominant blooming species (Fig. 5d). However, the files of individual FlowCam measurements can get quite big in the presence of large numbers of particles. Thus, it is common practice to use a digital size filter during image acquisition to exclude particle sizes that are presumably not of interest.

In our case, initially, we applied a digital size filter excluding particles  $<10~\mu m$  from being imaged. Midway through the experiment, we realized that this size fraction likely contained other bloom-forming species. When we removed the digital size filter, numerous small, round cells (< 10  $\mu m$ ) were indeed detected and subsequently identified as *Emiliania huxleyi* based on the presence of coccoliths.

To obtain a complete time series of the development of this species, we made two informed assumptions:

- 1. Particles in the 5–10  $\mu$ m size range primarily represent *Emiliania huxleyi* cells, as this range fits this species, and no other particle types were detected in this range in the FlowCam data once the size filter was removed
- 2. Particles in the 3–4 μm size range mainly represent detached coccoliths of *Emiliania huxleyi*

Under these assumptions, we employed the corresponding LISST-200X size-class data to track the temporal development of these two particle classes (representing *Emiliania huxleyi* and its coccoliths) over the course of the experiment (Fig. 5c). We observed a strong similarity between the 3–4  $\mu$ m particle trend (coccoliths)

and the development of the turbidity (Fig. 2b), thus suggesting that coccoliths were a major contributor to turbidity during the experiment. While other contributors cannot be entirely excluded, no additional particle types were clearly identifiable in our dataset.

We hope this clarifies the rationale behind our interpretation of the available data, and we have revised the manuscript text and Figure 5 caption accordingly.

Regarding SYBR Green labeling of bacterial cells, filtrating through 5 μm is not sufficient to prevent non-bacterial particles (e.g., coccoliths, picoeukaryotes, fungal spores, small organic flocs, etc.) from being analyzed. Additional validation is needed here. Furthermore, I have not received a response to my comment on the gating plots of the flow cytometry; since no other supporting analysis was performed, it is crucial to show the side and forward scatter gating used for counting bacterial cells, especially given that the bacterial counts are not typical for exponential growth, as seen in other mesocosm studies (see, for example, Vincent et al., 2023; https://doi.org/10.1038/s41467-023-36049-3).

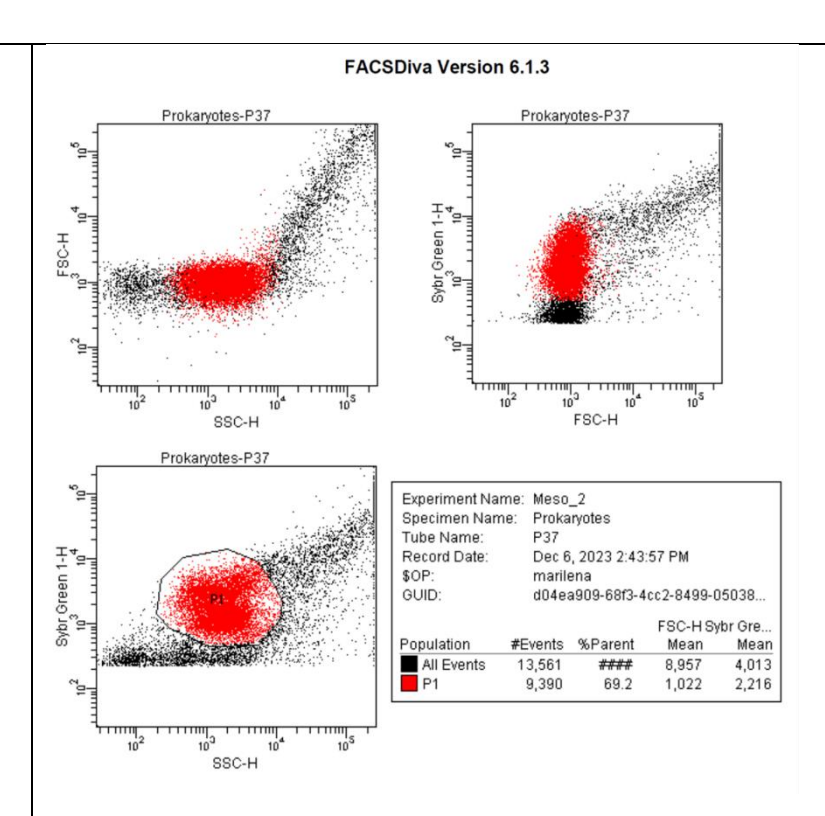
We agree that a 5  $\mu$ m prefiltration step alone does not entirely exclude all non-bacterial particles. This step was applied primarily to remove larger detrital aggregates and to prevent clogging of the flow cell.

To ensure that only bacterial populations were included in the analysis, we applied a stringent gating strategy based on SYBR Green fluorescence and side/forward scatter properties.

Representative gating plots have now been included in the Supplementary Material (Figs. S7 and S8) and also shown here as Figures R1 and R2.

In the revised manuscript, we have added the detailed description of the gating strategy based on SYBR Green fluorescence and side/forward scatter properties, together with its quality controls in the Methods section (Lines 281–299). We have also added the limitations of flow-cytometric counts in the discussion section (L792-797).

These additions provide visual confirmation that only nucleic-acidcontaining bacterial cells were counted and support the reliability of our gating approach.



of SYBR Green I-stained prokaryotic cells (gate P1, red) from background events. The panels display (top left) forward scatter (FSC-H) versus side scatter (SSC-H), (top right) SYBR Green I fluorescence (Sybr Green 1-H) versus FSC-H, and (bottom left) SYBR Green I fluorescence versus SSC-H. Gate P1 defines the population of nucleic-acid-containing bacterial cells based on characteristic fluorescence and scatter properties, excluding non-fluorescent debris and aggregates. The exact gate boundaries were applied to all experimental samples.

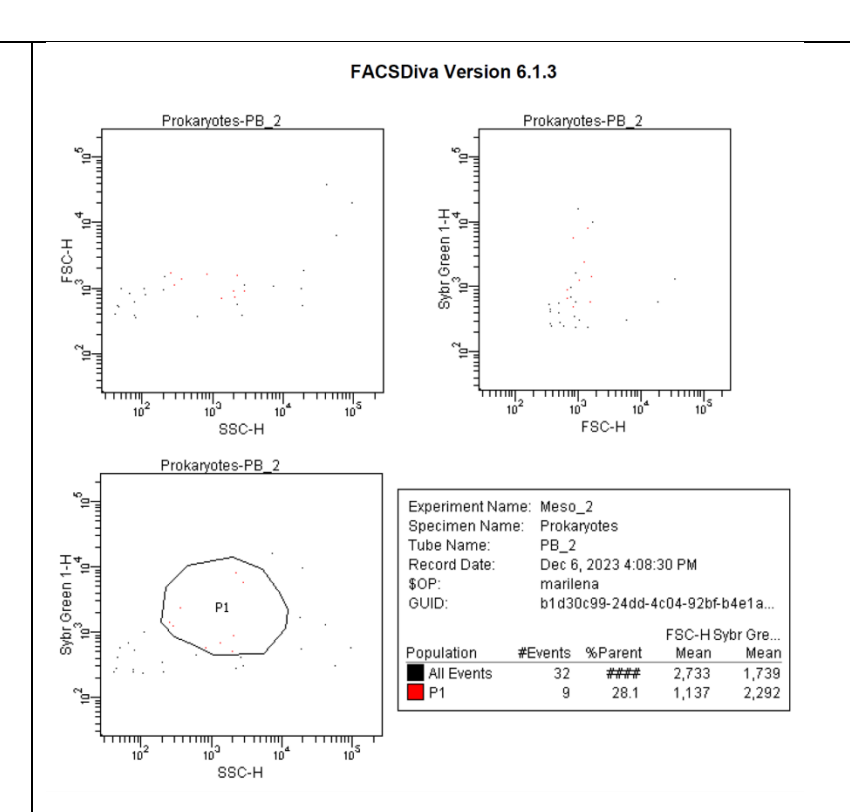


Figure R2. Flow-cytometric blank control for prokaryotic gating. Example of a Milli-Q water blank stained with SYBR Green I and processed under identical conditions as environmental samples. Very few events are detected within the prokaryotic gate (P1, red), confirming the absence of significant background fluorescence or particulate contamination. Panels show (top left) FSC-H versus SSC-H, (top right) SYBR Green I fluorescence versus FSC-H, and (bottom left) SYBR Green I fluorescence versus SSC-H. The blank served to define the fluorescence threshold and verify the specificity of the gating strategy for bacterial populations.

## **Note to the Editor and Referees**

As mentioned previously, the TDN dataset was undergoing re-evaluation. We replaced the TDN and DOC data based on the results of an interlaboratory comparison that revealed inconsistencies in the original measurements. The replacement analyses were conducted under standardized conditions at the GEOMAR laboratory. We have retained and present this corrected dataset in the main manuscript, as it enhances data reliability and is grounded in traceable, method-consistent reanalysis. This update does not affect the overall structure or conclusions of the study. A detailed explanation is provided in the Supplementary Material.